

Efficient Design Analysis of Chemical Sensor Using Hollow Core Photonic Crystal Fiber

Sandhir Kumar Singh*, Zeba Akhter & Md Tahseen Alam

Department of Sciences (Physics), IIIT Ranchi, Jharkhand 835 217, India

Received: 2 July 2024; accepted: 22 May 2025

Photonic Crystal Fiber (PCF) is an optical fiber, using a micro structural periodic arrangement of several air holes, which allows the broadband transmission and pulse propagation through it. Also, PCF has made the ideal functions for allowing the chemical sensing application, optical parametric calculation for telecommunication system. However, in some cases data transmission rate has minimized and signal loss has increased. Therefore, in this paper Hollow Core PCF (HC-PCF) based chemical sensor has been designed. The designed PCF geometry consists of symmetrical hexagonal air holes of three rings in the cladding and a hollow core region in the centre. Consequently, the designed PCF chemical sensor performance in methanol, ethanol, propanol and butanol have been analysed. Here, Finite Element Method (FEM) with Perfectly Matched Layer (PML) is used to analyse the guiding behaviour of the designed hollow core photonic crystal fiber (HC-PCF). Additionally, enhancement is made in various sensing function such as effective refractive index, spot size, confinement loss, power fraction, numerical aperture, V-parameter, non-linear coefficient and relative sensitivity. Consequently, the designed model has highest relative sensitivity and lowest confinement loss for various chemical analytes. Also, the developed model has numerically analysed and structured using COMSOL Multiphysics software.

Keywords: Photonic Crystal Fiber (PCF), Perfectly Matched Layer (PML), Hollow Core photonic crystal fiber (HC-PCF), Finite Element Method (FEM), Confinement loss (CL), Numerical aperture (NA), V-parameter, Refractive index (RI), Spot size, Relative sensitivity, Non-linear coefficient

1 Introduction

Over the past few decades, PCF technology has significant attention for extending the traditional optical fiber¹. Also, PCF has introduced a novel era to the enlargement of optical technology by permitting the fiber designs². Based on the light guiding mechanism the PCF has categorised into two types such as refractive index guiding PCF and photonic bandgap guiding PCF. PCFs are being investigated for their potential to carry data at higher capacities and over longer distances with reduced latency and minimum signal loss³. This is especially true for those with low-loss hollow cores⁴. As PCFs can accommodate many wavelengths at once, they are perfect for Wavelength Division Multiplexing (WDM) systems that increase the bandwidth of optical communication networks⁵. Because of their hollow core, PCFs are extremely sensitive to changes in refractive index because they can interact directly with gases and liquids⁶. They have a high specificity and sensitivity for the detection of chemical and biological materials. PCFs are used to monitor the quality of the air and water in real time by

identifying pollutants and dangerous materials in the environment⁷.

The capacity of PCF technology to increase interactions between light and analytes and to limit light has made it a power platform for chemical sensing⁸. A solid core with a regular pattern of air holes surrounding it allows light to be directed through it. It is possible to engineer these fibers with certain confinement and dispersion characteristics⁹. Light travels through a hollow core with an anti-resonant reflecting coating or a photonic bandgap structure encircling it on the principle of photonic bandgap guiding mechanism. The directed light and chemical analyte can interact directly in the hollow core¹⁰. It is possible to adjust the core's size, diameters of air holes and spacing between the consecutive air holes (pitch) to optimize the light-analyte interaction. Generally, smaller core sizes are more sensitive, but they can also cause more loss¹¹. The cladding's air holes size, shape, and arrangement control the PCF's sensitivity and guiding characteristics¹². For instance, it is possible to optimize a photonic bandgap structure to facilitate the propagation of particular wavelengths, improving the detection of particular substances¹³. To increase the

*Corresponding author: E-mail: sksingh@iiitranchi.ac.in

sensor's selectivity and sensitivity, compounds that preferentially bind to target analytes can be coated on the interior surfaces of the hollow core or the air holes in the cladding¹⁴. Identifying dangerous gases and pollutants including CO₂, CH₄, and NO_x this sensor can be used. Occupational safety to protect worker safety, hazardous gas detection is done in industrial settings¹⁵. Breath analysis looks for biomarkers in exhaled breath to provide non-invasive medical diagnosis¹⁶.

In optical communication systems, PCFs are used to control dispersion, lower signal loss, and increase data transfer speeds¹⁷. Additionally, because PCFs can direct light in air or gas-filled cores, improving interaction with the analytes and boosting sensitivity, they are used in chemical and biological sensing¹⁸. Furthermore, because of their high non-linearity and customized dispersion qualities, nonlinear optics are essential for producing light sources, optical parametric oscillation, and other nonlinear optical phenomena¹⁹. Additionally, PCFs are utilized in endoscopy, spectroscopy, and other imaging application in the medical and industrial domains²⁰. This is because of their capacity to direct light throughout a wide spectrum range and is difficult-to-access areas²¹. In previous, hexagonal structure with alcohol filled lattice PCF²², PCF fabrication strategy²³, silica fused hybrid PCF²⁴, drilling and stacking with temperature sensors²⁵, etc. these all are existing PCFs with complicated model. It has made fabrication complexity, requires higher cost, lower reliability, etc. so, a novel PCF based chemical sensors are designed to attain the higher selectivity and sensitivity for detecting various chemical substances.

Recent research has demonstrated remarkable progress in the design and optimization of HC-PCF sensors specifically for alcohol detection in the terahertz (THz) frequency range. Their innovative design, featuring rectangular air holes and an asymmetrical structure, not only enhances birefringence but also amplifies sensitivity, achieving performance levels that surpass existing methods. The sensor utilizes Zeonex as a base material, which contributes to its unparalleled sensitivity and minimal material loss, establishing new benchmarks for alcohol detection technologies.

2 Related Studies

Md Selim Hossen *et al.*,²⁶ have introduced the decagonal cladding based PCF to sense the chemicals in THz. Moreover, the sensor regions are created in Circular Air Holes (CAH) for evaluating the

performance of the sensors in terms of confinement loss (CL), sensitivity, etc. Consequently, core size, air hole length and pitch are the improvement parameters for the designed PCF. Also, these parameters are very important for sensing components as well as fabrication tolerance.

Highly sensible with modified hexagonal structure was designed by Islam *et al.*,²⁷ to demonstrate the model analysis of PCF. Also, numerical investigation has carried with perfect match layers using full vector finite element analysis. Here, liquid analyser was used to filter out the fibre core. Then, relative sensitivity is assessed by varying the parameter with wavelength up to 1.0 to 1.7 μm . Consequently, the developed design structure has higher sensitivity in terms of all alcohol analytes and 9.33×10^{-11} dB/m confinement loss which is lower at wavelength of 1.55 μm .

To sense the biochemical application Maida *et al.*²⁸ have designed the germanium doped solid core PCF. PCF based sensor have been developed to analyse the blood parameters such as plasma, red blood cell, white blood cell, water and haemoglobin. Here, these analysis process were done using COMSOL Multiphysics tool. The simulation parameter is 1.3 μm wavelength, with higher relative sensitivity. Moreover, the developed design has attain better performance in terms of beam divergence, confinement loss, propagation constant and spot size.

3 Design Methodology

This study has developed a Hollow-core PCF with FEM for chemical sensor to enhance the sensitivity as well as reduce the confinement loss. Moreover, Hollow core PCF can deals chemical sensing performance with strong platform due to their unique ability and geometry to guide the minimal loss through the hollow core analytes. Moreover, the developed design is functioned as particular application for making various fields such as industrial process, environmental monitoring and medical diagnosis. Consequently, in a hollow core structure the core is generally filled with liquid or gas, which is significantly enhance the interaction length with the light as compared with the traditional solid core fibres. This would exhibit under lower attenuation over a long distance for allowing the low detection concentration of chemical reactions. Here, conducted the numerical simulation and experimental analysis for estimating the performance of designed fiber. Therefore, the designed structure was performed in two way such as numerical analysis and chemical sensor geometry.

3.1 Chemical Sensor

The HC-PCF sensor working principle has involved three main functions, such as, affecting the optical signal, propagation core region and analysing substance. Because, PCF is the most important element which can extended to analyse the detection performance. Here, the HC-PCF consists of cladding air holes, which is the essential process to keep the core region lightening at optimal interaction. Moreover, Fig.1 demonstrates structure of developed chemical sensor HC-PCF design. Consequently, the design consists of three layers such as Perfectly Matched Layer (PML), cladding with air hole and finally core infiltrated with liquid. Here, the leakage wavelength are observed with the help of PML also; it can prevent the light reflection of the cladding at back region. Then, the core used to conduct the light and core is responsible to restrict the light inside the core region. The developed HC-PCF design is for chemical sensing which is located in hollow circular hole of the fiber core. Then, the air holes are distributed over the cladding and outermost has three rings which consist 54 circular air holes. The first ring closest to the core has 12 circular air holes with a diameter of d_1 , spaced equally at a distance of P_1 . The second ring has 18 circular air holes with a diameter of d_2 and a distance of P_2 between two consecutive air holes. The third ring has 24 circular air holes with a diameter of d_3 and a distance of P_3 between two consecutive air holes. Beyond the cladding zone, a PML is employed to stop wandering waveguides from reflecting onto the fiber. By employing round holes, which are thought to be easy to make, the suggested PCF design seeks to develop a fiber that is simple to manufacture. The diameter and pitch size (distance between two consecutive air holes in a ring) of these holes are modified to the proper dimensions prior to the design being finalized.

Moreover, PML has adjusted with equivalent size with 105 of cladding diameter and circular holes are filled with different liquid analytes. Design parameter with specified values are enclosed in Table 1.

3.2 Numerical Assessment

Here, the separate liquid is fed into the core of HC-PCF. Sellmeier’s equation is used to calculate the

effective refractive indices(η_{EFF}), which is mentioned as:

$$\eta_{EFF}(\lambda) = \sqrt{1 + \frac{b_1\lambda^2}{\lambda^2 - c_1} + \frac{b_2\lambda^2}{\lambda^2 - c_2} + \frac{b_3\lambda^2}{\lambda^2 - c_3}}$$

where, b_i and c_i is represented as Sellmeier coefficient with ($i=1, 2, 3$) and λ denoted as working wavelength (Table 2). Then, to find the detection ability of PCF sensor by comparing the relative sensitivity with refractive indices for surrounding medium mathematical modelling is required. Consequently, effective refractive index is wavelength

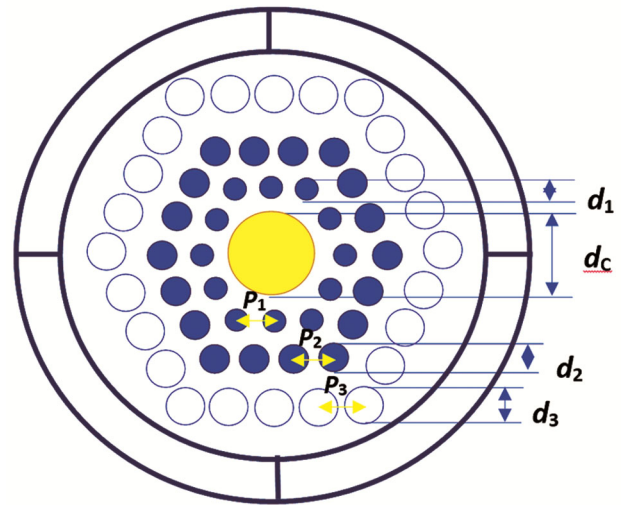


Fig. 1 — Structure of HC-PCF

Table 1 — Design parameters

Specification of geometrical parameters of designed HC-PCF	Measurement in (μm)
Diameter of air holes in first ring	$d_1 = 0.5\mu m$
Pitch of first ring (distance between two consecutive air holes of first ring)	$P_1 = 2.2\mu m$
Diameter of air holes in second ring	$d_2 = 0.8\mu m$
Pitch of second ring (distance between two consecutive air holes of second ring)	$P_2 = 1\mu m$
Diameter of air holes in third ring	$d_3 = 2\mu m$
Pitch of third ring (distance between two consecutive air holes of third ring)	$P_3 = 0.7\mu m$
Circular core diameter (centre)	$d_c = 4.1\mu m$
Total diameter of the fiber (with boundary criteria)	$24\mu m$

Table 2 — Values of Sellmeier coefficients for different analytes

Analytes	Sellmeier coefficients				
	a	b	c	d	x
Butanol	0.00115077	0.01373734	0.00194084	0.000254077	1.917816501
Propanol	0.003349425	0.004418653	0.00108023	0.000067337	1.893400242
Ethanol	0.83189	0.00930	-0.15582	49.45200	N/A
Methanol	0.00536218	0.004656355	0.00044714	0.000015087	1.745946239

dependent and constants values, so the refractive indices for wavelength value are derived in following Eq (1-4), for methanol, ethanol, propanol and butanol analytes respectively.

$$M_n(\lambda) = \sqrt{x - a\lambda^2 + \frac{b}{\lambda^2} + \frac{c}{\lambda^4} - \frac{d}{\lambda^6}} \quad \dots (1)$$

$$E_n(\lambda) = \sqrt{1 + \frac{a\lambda^2}{\lambda^2 - b} + \frac{c\lambda^2}{\lambda^2 + d}} \quad \dots (2)$$

$$P_n(\lambda) = \sqrt{x - a\lambda^2 + \frac{b}{\lambda^2} + \frac{c}{\lambda^4} - \frac{d}{\lambda^6}} \quad \dots (3)$$

$$B_n(\lambda) = \sqrt{x - a\lambda^2 + \frac{b}{\lambda^2} - \frac{c}{\lambda^4} + \frac{d}{\lambda^6}} \quad \dots (4)$$

where, a, b, c, d and x are the constant coefficients and the finding mainly based on the amount of light interact with surrounding medium.

So, to find the relative sensitivity using Eq (5),

$$S_r = \frac{\eta_{analyte}}{\eta_{EFF}} \times f\% \quad \dots (5)$$

where, S_r , $\eta_{analyte}$ and η_{EFF} denotes the relative sensitivity, effective refractive index of the analyte and guided mode respectively. Here f defines the light signal amount over the core known as power fraction. Here, power fraction is termed as ratio of chemically loaded region and to the total power in the whole fiber. Moreover, the power fraction parameter is calculated based on the integration function. Also, the power fraction metric denotes the amount of energy transmitted to the PCF with given location. Here, Poynting's theorem is applied to solve this criteria using Eq (6),

$$f = \frac{\int \text{Re}(e_x m_y - e_y m_x) dx dy}{\int_{total} \text{Re}(e_x m_y - e_y m_x) dx dy} \times 100 \quad \dots (6)$$

where, $e_x m_y$ and $e_y m_x$ is denoted as electric and magnetic fields of the transverse guided mode. According to this statement, the denominator of the equation includes the entire fiber, whereas the integral in the numerator covers the area of the fiber where the analyte is present, which means the core of the fiber. Moreover, confinement loss (CL), or light leaking from the core into the cladding zone, is depicted in the PCF design. This CL is caused by structural characteristics of the fiber. The imaginary component

of the complex effective index must be calculated in order to get the CL. Consequently to find the confinement loss using Eq (7),

$$CL = 8.686 \times \frac{2\pi f_0}{c} \text{Im}(\eta_{EFF}) \text{ (dB/cm)} \quad \dots (7)$$

Where f_0 and c denotes the operating frequency and speed of the light of PCF respectively and $\text{Im}(\eta_{EFF})$ is the imaginary part of effective refractive indices of the fundamental mode. After finding the CL the fiber core's effective area is evaluated. Cross sectional area of the PCF and transverse electric vectors are used to find the effective area of the fiber core. Here, effective mode area is strongly correlated with the effective area of the fiber core. Moreover, this is the most important region to transport the light. Consequently, effective area (a_{eff}) of the fiber core is calculated using Eq (8),

$$a_{eff} = \frac{(\iint_{-\infty}^{\infty} |e|^2 dx dy)^2}{\iint_{-\infty}^{\infty} |e|^4 dx dy} \quad \dots (8)$$

where, e represented as transverse electric field vector. Moreover, the developed system needs high bit rate for transmitting the data from large effective mode areas. Here, non-linear coefficient function was directly related to the effective area of the fiber. Then, estimate the light intensity measurement using Eq (9),

$$\varepsilon = \left(\frac{2\pi}{\lambda}\right) \left(\frac{n_l}{a_{eff}}\right) \quad \dots (9)$$

where, n_l is denoted as non-linear refractive index,

4 Result and Discussion

To evaluate the efficiency of the newly designed Hollow Core PCF its several parameters are analysed such as power fraction, confinement loss, relative sensitivity, non-linearity and effective area in terms of all alcohol analytes. The interaction of light occurs in the core region of the fiber at an operating wavelength of 1.3 μm , and the mode field is fully contained within the four test analytes, which are methanol, ethanol, propanol and butanol. The efficiency of the suggested design in steering waves is generally confirmed by the notable confinement of light within the centre of a single air hole. In addition, the intense interaction between light and analytes suggested by this confinement is important for attaining high sensitivity in liquid detection. Achieving the optimal alignment between the guided modes and the infiltrated liquids can maximize their overlap by optimizing the power fraction and intensity within the hollow core.

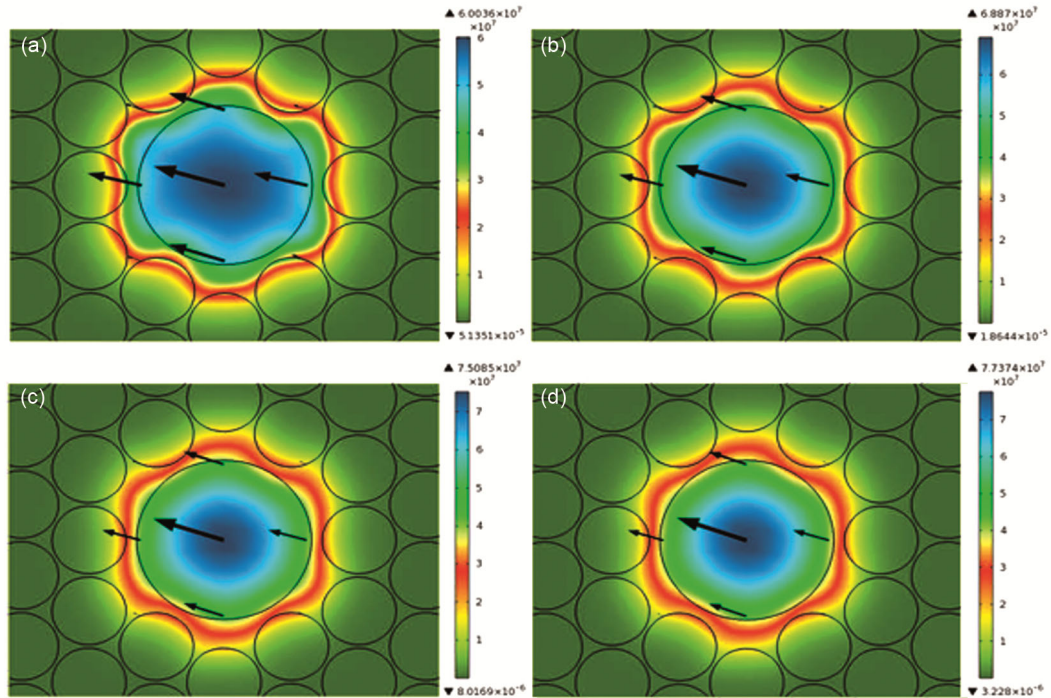


Fig. 2 — The developed sensor mode with field distribution of (a) Methanol, (b) Ethanol, (c) Propanol, and (d) Butanol

Figure 2 shows the electromagnetic signal propagation properties for all alcohol analytes. This image makes it clear that, for all analytes, the electromagnetic pulse is tightly contained within the core area. Furthermore, the picture indicates that among the tested analytes, butanol has the highest effective refractive index and methanol has the lowest, indicating that butanol has the largest light confinement.

4.1 Performance Evaluation

To validate our proposed model in the analysis of performance metrics are evaluated in standings of effective refractive index, spot size, confinement loss, power fraction, numerical aperture, V-parameter, non-linear coefficient and relative sensitivity.

4.1.1 Refractive Index

Effective refractive index is the most fundamental parameter in PCF which controls the light propagation through the fiber. Moreover, the experimental outcomes shows that when the operating wavelength increases, simultaneously effective refractive index of the material decreases. With Chromatic dispersion and theoretical predictions effective refractive index is termed as consistent. Moreover, optical materials has reduces the effective refractive index because of the longer wavelengths. During the dispersive nature, the PCF configuration can interact between the matter and

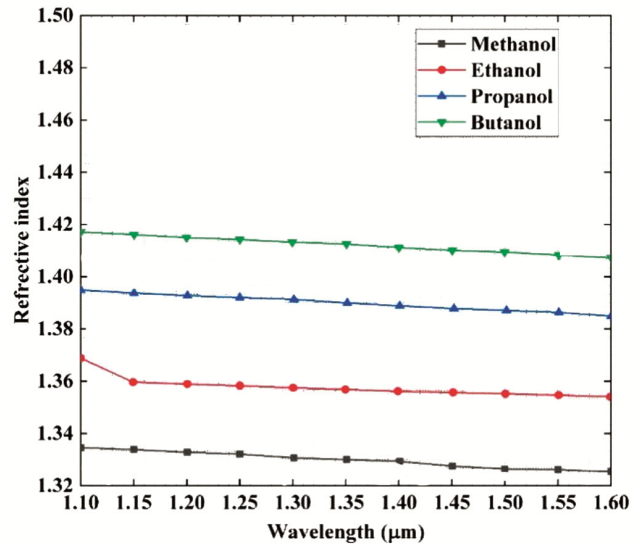


Fig. 3 — Refractive index of various analytes with wavelength

light based on the tiny electromagnetic wave propagation. Also, the effective refractive index is decreased due to the presence of tiny air holes in the cladding. This phenomenon done through the higher refractive index region. Figure 3 illustrates graphical demonstration of refractive index of methanol, ethanol, propanol, and butanol with varying wavelength. Butanol shows highest refractive index than other analytes.

4.1.2 Relative Sensitivity (%)

The most important factor for understanding the accurate characteristics for sensor's are termed as relative sensitivity. Moreover, this parameter, which can be found using the Beer-Lambert law, which indicates the interaction between the testing analyte at a specific wavelength and the propagating electromagnetic signal of the developed sensor. Additionally, the electromagnetic signal's preference for propagating within the higher refractive index analyte is butanol. Figure 4 shows, relative sensitivity for butanol is higher than any other alcohol analytes due to its highest refractive index than other one.

4.1.3 Numerical Aperture

Numerical Aperture is one of the important parameter for evaluating the performance of the developed PCF. The highest incident light angular acceptance that can go through the fiber is indicated by numerical aperture. Moreover, this parameter is mainly dependent on the structure of air holes as well as geometric arrangement. The calculation of numerical aperture is mentioned in Eq (10),

$$NA = \frac{1}{\sqrt{1 + \frac{\pi a_{eff} f^2}{c^2}}} \approx \frac{1}{\sqrt{1 + \frac{\pi a_{eff}}{\lambda^2}}} \quad \dots (10)$$

where, incident light frequency is denoted as f and a_{eff} is represented as effective area which can propagate the electromagnetic signal. Numerical aperture is limited between zero to unity and this limit is efficient for desired system with various operating wavelengths. Moreover, developed PCF with various operating wavelengths of the NA parameter is illustrated in Fig.5. The attained outcomes that have been clarified shows that when the signal's wavelength grows, NA climbs. This happens when the wavelength square eventually lowers the denominator, but only marginally improves the effective area at higher wavelengths. Because methanol has a smaller effective area than other alcohols, it has the largest numerical aperture under fixed conditions. The numerical apertures of methanol, ethanol, propanol, and butanol are 0.412, 0.382, 0.362 and 0.344, respectively as shown in the Fig. 5 at 1.3 μm wavelength and at fixed power fraction (p) of 1.4 μm , respectively.

4.1.4 V-parameter

The proportion of the PCF's overall area that is occupied by the core and cladding air holes is

estimated, together with the PCF's overall area. Here, the simple mathematical modelling is used to estimate the value of cladding refractive index in developed PCF. Initially, the cladding air holes and total area of the PCF in term of PCF's overall area is estimated. The received light exhibits no modal distortion, and this fiber is regarded as a single-mode fiber. Using the following Eq (12) the v-parameter is quantified.

$$V = \frac{2\pi}{\lambda} \Lambda \sqrt{n_{eff,core}^2 - n_{eff,clad}^2} \quad \dots (11)$$

where, $n_i(co)$ is denoted as refractive index of core and $n_i(cl)$ refractive index of cladding. Here, the fiber will only allow one mode to pass through it if the parameter value is less than or equal to 2.405. The received light exhibits no modal distortion, and this

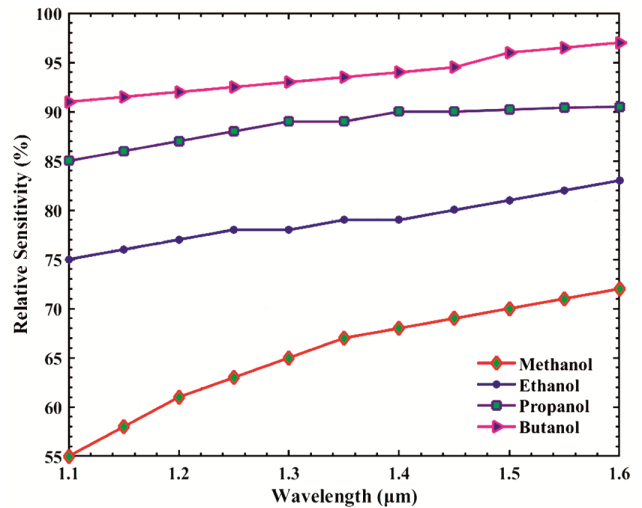


Fig. 4 — Relative sensitivity with wavelength ($\lambda = 1.1 - 1.6 \mu\text{m}$)

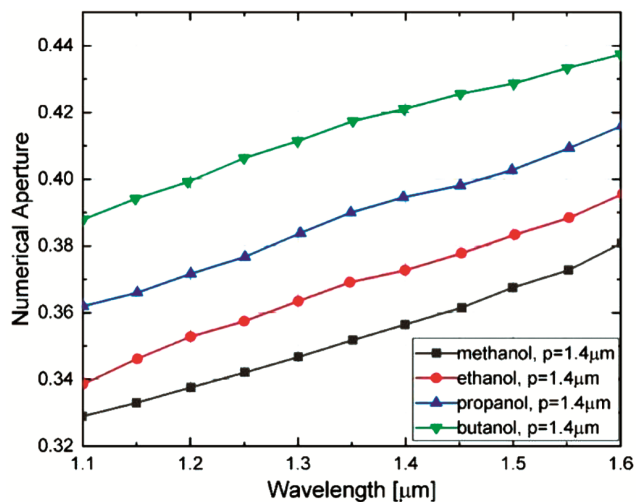


Fig. 5 — Variation of Numerical aperture with wavelength for different electrolytes at fixed power fraction ($p=1.4\mu\text{m}$)

fiber is regarded as a single-mode fiber. Figure 6 illustrates the performance of V-parameters of methanol, ethanol, propanol, and butanol with wavelength.

4.1.5 Power Fraction

It shows that when the wavelength increases, the power fractions of methanol and ethanol rise at about $1.0\mu\text{m}$ and then progressively fall. On the other hand, butanol power fraction drops with wavelength $1.1\mu\text{m}$, suggesting that it is less sensitive to longer wavelengths. These discoveries can help with developed PCF sensor design and optimization for these chemical related applications. The power fractions at $1.3\mu\text{m}$ for methanol, ethanol, propanol, and butanol are 98.7%, 97.8%, 95.7% and 96.8% respectively, which is illustrated in Fig.7. These discoveries are crucial for a number of applications, including environmental monitoring and medical diagnostics, where the detection of these chemicals is crucial. The power fraction trends illustrate how wavelength affects sensitivity and how to determine the ideal operating point. Greater power fractions indicate that more light is being trapped in the core and interact with the injected analytes. This facilitates the observation of minute variations in the liquids. From the graphical representation power fraction is decreased with the increasing wavelength from $1.1\mu\text{m}$ to $1.6\mu\text{m}$. Moreover, at higher wavelengths the operational wavelength moves closer to the edge of the bandgap, the power fraction in the core can decrease due to less effective confinement. Consequently, shorter wavelengths can push the operating wavelength deeper into the bandgap region, potentially increasing the power fraction in the core due to better confinement. Also, losses increase at shorter wavelengths, reducing the power fraction in the core.

4.1.6 Confinement Loss

Confinement loss of the proposed PCF varies with different wavelength for the methanol, ethanol, propanol, and butanol. Here, the wavelength increases, confinement loss of the four liquids increases by passing the more light to the cladding and leave the core.

The values that are attained represent the extent to which the PCF sensor can contain light inside the core and stop it from escaping. Greater light guidance over longer distances with less light leaking into the cladding is made possible by lower loss. This enhances the sensitivity of the detection by enabling

more interactions with the infiltrating analytes. The findings imply that the suggested PCF sensor might be beneficial in a variety of sensing applications and might be efficient in identifying and analysing the characteristics of methanol, ethanol, propanol, and butanol. Here, the confinement loss with varying wavelength curve is demonstrated in Fig. 8. Consequently, power fraction increases with varying the wavelength from $1.1\mu\text{m}$ to $1.6\mu\text{m}$. Moreover, the wavelength is $1.2\mu\text{m}$ confinement loss of methanol, ethanol, propanol, and butanol was slowly reduced but the wavelength level exceeds $1.3\mu\text{m}$ confinement loss increased too fast. So, the developed PCF has better performance compared to other liquid sensors at $1.3\mu\text{m}$ wavelength.

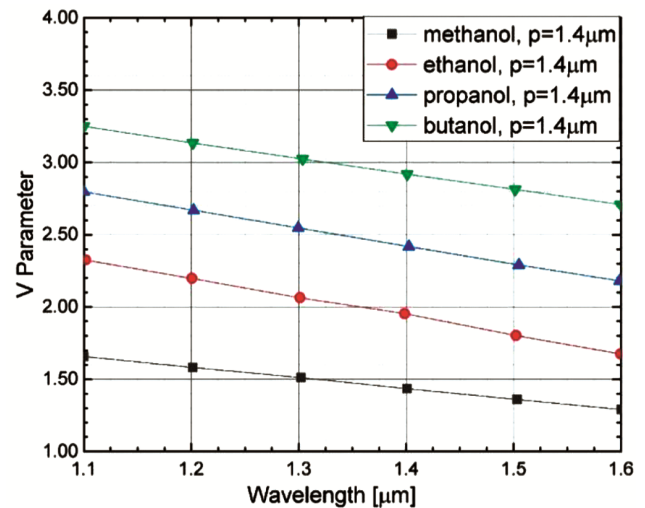


Fig. 6 — Performance of V-parameter with wavelength at fixed power fraction ($p=1.4\mu\text{m}$)

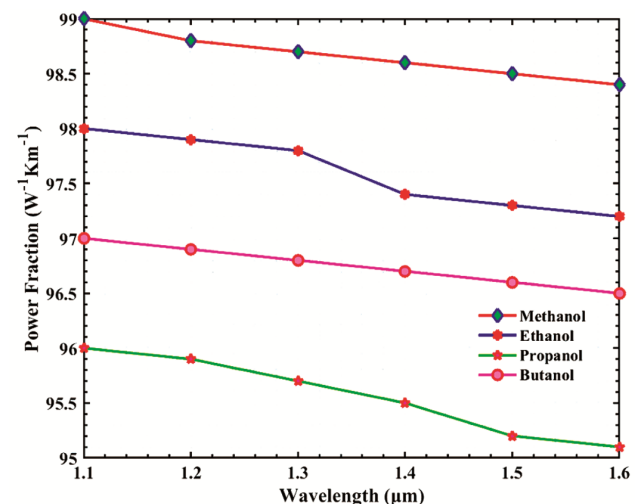


Fig. 7 — Performance of power fraction for different electrolytes with wavelength

4.1.7 Spot Size

When developing the optical fiber-based systems, spot size is a crucial consideration because the V-parameter and this spot size parameter are tightly connected to each other. A larger spot size value is preferable for various sensing application. Because, the spot sizes for methanol, ethanol, propanol, and butanol increases steadily from 1.1 μm to 1.6 μm wavelength, as is shown in Fig. 9.

The spot size features are nearly reversed because the spot size and the V parameter have an inverse

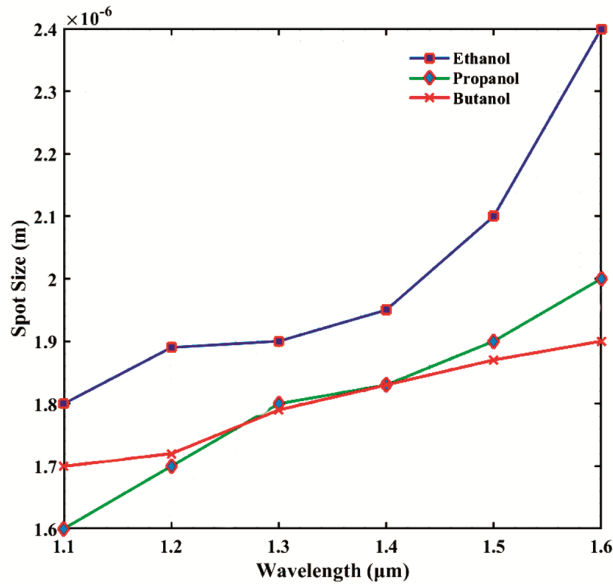


Fig. 8 — Confinement loss with wavelength for different electrolytes for developed PCF

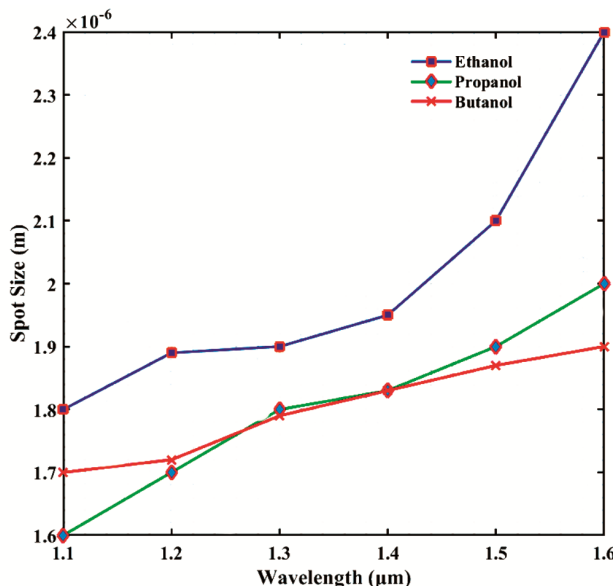


Fig. 9 — Spot size performance with wavelength for different electrolytes

relationship. Under ideal geometry and wavelength conditions, the suggested sensor provides a spot size of 1.9×10^{-6} μm , 1.8×10^{-6} μm and 1.78×10^{-6} μm for ethanol, propanol, and butanol, at 1.3 μm wavelength respectively.

4.1.8 Non-Linear Coefficient

Figure 10 shows a graphical illustration of the relationship between the operating wavelength and the liquid analytes nonlinear coefficients. Similar behaviours are seen in methanol, ethanol, propanol and butanol; as the operating wavelength increases, the nonlinear coefficient decreases. The effective area and the nonlinear coefficient, however, have a contradictory connection. At a wavelength of 1.3 μm , the nonlinearity coefficients of methanol, ethanol, propanol, and butanol are nearly the same, with values of 30, 27, 22 and 20 $\text{W}^{-1} \text{km}^{-1}$, respectively, which is demonstrated in Fig. 10. By mitigating these impacts, PCF sensors can provide more accurate and consistent data.

Moreover, at shorter wavelengths the effective mode area is smaller due to tighter mode confinement. This results in a higher nonlinear coefficient because the mode area is smaller. Then the shorter wavelengths can enhance nonlinear interactions because of stronger mode confinement and higher power density. Wavelength decreases, the effective mode area becomes smaller, leading to a higher nonlinear coefficient. This enhances nonlinear interactions.

5 Discussion

The proposed PCF was designed with a fairly simple layout for use in liquid sensing applications. It

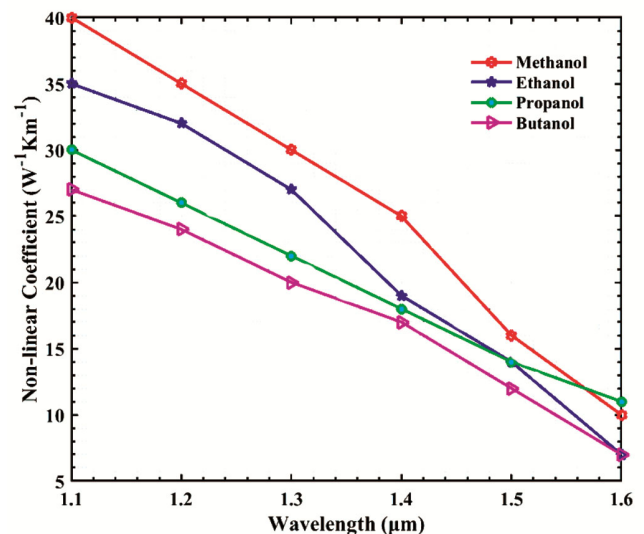


Fig. 10 — Non-linear coefficient of developed PCF sensor with wavelength

Table 3 — Comparative analysis

Reference	Material	Samples	Relative sensitivity (%)	Confinement loss (dB/m)	Power fraction	Numerical aperture	Refractive index	v-parameter	Non-linear coefficient	Spot size
[30]	Fused silica	water	96.84	1.2×10^{-2}	92	-	1.3	-	13.98	-
		Ethanol	98.12	1.5	94	-	1.34	-	13.93	-
		benzene	99	1.0	98	-	1.45	-	14.85	-
[29]	Fused silica	water	94.47	7.31	82	-	1.28	-	-	-
		Ethanol	96.32	3.70	90	-	1.33	-	-	-
		benzene	99.63	1.76	96	-	1.45	-	-	-
Proposed	Fused silica	Methanol	65	10^{-12}	98.7	0.412	1.33	1.4	30	-
		Ethanol	78	10^{-13}	97.8	0.382	1.35	2.3	27	2.4
		Propanol	88	10^{-13}	95.7	0.362	1.47	2.7	22	1.9
		Butanol	92	10^{-13}	96.8	0.344	1.49	3.2	10	1.8

has one core hole and fifty four cladding air holes. With the current advancements in fabrication technology, it is easy and affordable to create anything with such a basic design. Despite these advantages, it has been shown that the sensitivity of the proposed PCF is higher than several PCFs with more complex designs.

A comparison of the suggested PCF and previously studied chemical PCF sensors is shown in Table 3. The findings unambiguously show that the suggested PCF performs better in terms of relative sensitivity and confinement loss. The data displayed in the Table 3 indicates that, in comparison to other sensors, the recommended PCF sensor has the better relative sensitivity. It also shows a minimal degree of confinement loss.

6 Conclusion

PCF is the recently developed optical fiber which shows the effective performance for sensing the liquid in lower wavelength range. Moreover, liquid sample identification and quantification is the most important performance for monitoring laboratory research, medical diagnosis, environmental conditions, etc. here, this paper designed a novel PCF based HC structure with cladding air holes and core holes in hexagonal structure. This design has effectively allows the various detection performance. Also, FEM was applied to conduct the simulation study in terms of numerical analysis. Here, methanol, ethanol, propanol and butanol are different liquids that can used to test the PCF characteristics. The outcomes

demonstrates that the developed PCF has higher relative sensitivity of 65%, 78%, 88% and 92% respectively and the non-linearity coefficient of 30, 27, 22 and 20 $W^{-1}Km^{-1}$ for methanol, ethanol, propanol and butanol respectively at wavelength 1.3 μm . Also, it has better performance outcomes in dealing with power fraction, confinement loss, numerical aperture, refractive index, etc. This indicates that the suggested fiber may find use in a number of fields, such as chemical detection, optical communication, and bio-sensing. All things considered, the PCF is a promising invention that can help progress the field of liquid sensing and open the door to new technological applications.

References

- 1 Jibon R H, Khodaei A, Priya P P, Rashed A N Z, Ahammad S H & Hossain M A, *Opt Quant Electron*, 55, 2023.
- 2 Bulbul A A M, Podder E, Ahammad S H, Faragallah O S, Eid M M A & Rashed A N Z, *J of Comput Electron*, 22 (2023) 1725.
- 3 Kundu D, Hossain M S, Thanga L, Sahoo S, Karthikeyan S, Ramkumar G, Gopalan A, Prakash P, Ferdous A H M I, Hossain S & Rashed A N Z, *Plasmon*, 2024.
- 4 Moeglen Paget B, Vinod Ram K, Zhang S, Perumal J, Vedraïne S, Humbert G, Olivo M & Dinis U S, *Sensors and Actuators B: Chem*, 400 (2024) 134828.
- 5 Al Mahmud M A, Islam M R, Iftekher A N M, Rahman M M & Mou F A, *Microsystem Technol*, 29 (2022) 115.
- 6 Luo W, Abbasi W A, Li X, Ho H P & Yuan W, *Plasmon*, 2024.
- 7 Ehyae A, Mohammadi M, Seifouri M & Olyae S, *Euro Phys J Plus*, 138, 2023.
- 8 Zhang Z, Li S, Yin Z, Ullah S, Cui X, Li G, Li K, Wang C and Liu Y, *Plasmonics*, 19 (2023) 495.

- 9 Ferdous A H M I, Noor K S, Balamurugan K, Ramkumar G, Kumar C R, Mohan S B, Xavier B M, Hossain M S, Noor S Z E, Sathi B N, Rashed A N Z & Hossain A, *J Opt*, 2023.
- 10 Xu L, Liu C, Shi Y, Yi Z, Lv J, Yang L, Wang J & Chu P K, *Optik*, 286 (2023) 170941.
- 11 Habib M A, Anower M S, AlGhamdi A, Faragallah O S, Eid M M A & Rashed A N Z, *Optical Review*, 28 (2021) 383.
- 12 Sardar M R, Faisal M & Ahmed K, *Sens Bio-Sens Res*, 31 (2021) 100401.
- 13 Senthil R, Anand U & Krishnan P, *Appl Phys A*, 127, 2021.
- 14 Yang J, Shen R, Yan P, Liu Y, Li X, Zhang P & Chen W, *Sensors and Actuators B: Chem*, 306 (2020) 127585.
- 15 Eid M M A, Habib M A, Anower M A & Rashed A N Z, *Brazilian J Phys*, 51 (2021) 1017.
- 16 Habib A, Anower S & Haque I, *Sensors Int*, 1 (2020) 100011.
- 17 Eid M M A, Habib M A, Anower M S & Rashed A N Z, *Microsys Technol*, 27 (2020) 1007.
- 18 Paul A K, Samiul Habib M, Hai N H & Abdur S M Razzak, *Opt Comm*, 464 (2020) 125556.
- 19 Hossain M S, Kamruzzaman M M, Sen S, Azad M M & Hossain Mollah M S, *Sens Bio-Sens Res*, 32 (2021) 100426.
- 20 Islam M N, Al-tabatabaie K F, Habib M A, Iqbal S S, Qureshi K K & Al-Mutairi E M, *Crystals*, 12 (2022) 1362.
- 21 Luo Y, Fan R, Zhang Y, Wu Q, Ren Z & Peng B, *Opt Fiber Technol*, 48 (2019) 278.
- 22 Hu D J J, Lim J L, Cui Y, Milenko K, Wang Y, Shum P P & Wolinski T, *IEEE Photon J*, 4 (2012) 1248.
- 23 Falkenstein P, Merritt C D & Justus B L, *Opt Lett*, 29 (2004) 1858.
- 24 Islam M S, Sultana J, Dinovitser A, Ahmed K, Ng B & Abbott D, *Opt Comm*, 426 (2018) 341.
- 25 Habib M A, Reza M S, Abdulrazak L F & Anower M S, *Opt Comm*, 446 (2019) 93.
- 26 Hossain M S, Hossen R, Alvi S T, Sen S, Al-Amin M & Hossain M M, *Physics Open*, 17 (2023) 100168.
- 27 Islam M S, Paul B K, Ahmed K, Asaduzzaman S, Islam S, Chowdhury S, Sen S & Bahar A N, *Alexand Engg J*, 57 (2018) 1459.
- 28 Maida A M, Kalam M A & Begum F, *Sens Bio-Sens Res*, 41 (2023) 100565.
- 29 Maida A M, Shamsuddin N, Wong W R, Kaijage S & Begum F, *Photon*, 9 (2022) 38.
- 30 Jebur R S & Thaher R H, *Open Engg*, 14 (2024).